Contemporary Mathematics
http://ojs.wiserpub.com/index.php/CM/

UNIVERSAL WISER PUBLISHER

Research Article

Advancing Computational Insights: Domination Topological Indices of Polysaccharides Using Special Polynomials and QSPR Analysis

Suha Wazzan[1*], **Hanan Ahmed**[2]

[1]Department of Mathematics, Science Faculty, King Abdulaziz University, Jeddah 21589, Saudi Arabia
[2]Department of Mathematics, Ibb University, Ibb 70270, Yemen
E-mail: swazzan@kau.edu.sa

Received: 23 July 2023; **Revised:** 10 September 2023; **Accepted:** 21 September 2023

Abstract: Topological indices play a pivotal role in deciphering the structural and physicochemical properties of complex molecular structures, especially polysaccharides like amylose and blue starch-iodine compounds. However, accurately determining these indices for such compounds, considering their diverse isomeric forms, has been a persistent challenge. While various methodologies have been proposed in the literature, many fall short in versatility, often failing to provide comprehensive correlations with physicochemical properties. Addressing this gap, our study introduces a pioneering approach using $\varphi_{\mathfrak{R}}$-polynomial and φ_{γ}-polynomial methodologies. This novel method not only encompasses both chair and boat isomeric forms but also integrates density functional theory (DFT) calculations utilizing the *DFT/TPSSTPSS/cc-pVTZ* basis set within the Gaussian 09 software. To validate our approach, we conducted a quantitative structure-property relationship (QSPR) analysis and juxtaposed our findings with renowned compounds like nicotine and aspirin. The results unveiled robust correlations between the topological indices and the intrinsic properties of the compounds, underscoring the efficacy and reliability of our methodology. This research not only augments our comprehension of polysaccharides but also illuminates potential applications spanning pharmaceuticals, materials science, and agriculture. Furthermore, the compelling correlations observed herald the potential for the innovative design of new polysaccharides with tailored properties.

***Keywords*:** domination topological indices, polysaccharides, QSPR analysis, M-polynomials

MSC: 05C05, 05C12, 05C90

1. Introduction

In the realm of molecular science, understanding the intricate properties and behaviors of complex molecules is paramount. With the advent of computational tools, researchers have been able to delve deeper into the mysteries of molecular structures, leading to groundbreaking discoveries in various fields [1]. Among these molecules, polysaccharides stand out due to their multifaceted roles in living organisms, from energy storage mechanisms to providing structural support [2]. Among all nutritional polysaccharides, amylose is the most basic, consisting purely of glucose polymers connected only by α(1-4) bonds. Starch is a mixture of amylose and amylopectin.

In contrast to amylopectin, amylose cannot be dissolved in water and is harder to digest. Another view of amylose digestibility and solubility is seen in its complexion. The structure of amylose, along with its slow breakdown mechanisms, plays an important role in storing plant energy in the process of photosynthesis. Polysaccharides also

Copyright ©2023 Suha Wazzan, et al.
DOI: https://doi.org/10.37256/cm.5120243419
This is an open-access article distributed under a CC BY license
(Creative Commons Attribution 4.0 International License)
https://creativecommons.org/licenses/by/4.0/

provide structural support for cells. Besides, hemicelluloses are another group of polysaccharides located in plant cell walls. In 1814, Colin and Claubry made the discovery of the starch-iodine reaction, known to every chemist from his introductory courses in quantitating and qualitative analysis [3, 4].

However, comprehending the nuances of these biomolecules requires sophisticated mathematical descriptors and computational methodologies. Computational chemistry and bioinformatics have emerged as indispensable tools in this endeavor, offering a lens through which the properties of polysaccharides can be viewed and understood [5]. One such mathematical descriptor, the domination topological indices, has proven to be particularly insightful, revealing the structural and topological properties of molecules [6].

Many studies on topological indicators have been conducted in various fields of molecular graphs and networks, with a variety of indicators having been created and developed (see examples in [7-11]). In recent work, Wazzan et al. [12], presented a detailed investigation into symmetry-adapted domination indices, particularly focusing on the enhanced domination sigma index (EDSI). Through its application in quantitative structure-property relationship (QSPR) studies of octane and its isomers, they seek to highlight the potential of EDSI in understanding complex molecular structures and predicting their physicochemical properties. This research contributes to the expanding field of topological indices and sets the stage for future advancements in molecular design and material development.

Let ζ be a connected simple graph with $V(\zeta)$, a set of vertices and $E(\zeta)$, a set of edges. A set $D \subseteq V$ is said to be a *dominating set* of a graph ζ, if for any vertex $v \in V-D$, there is a vertex $u \in D$ such that u and v are adjacent. For more details on domination in graphs, (see examples in [13-16]). A dominating set $D = \{v_1,v_2,...,v_r\}$ is minimal if $D - v_i$ is not a dominating set [17]. A dominating set of ζ of minimum cardinality is said to be a minimum dominating set. In [18], Shashidhara et al. have introduced new degree-based topological indices called domination topological indices, which are based on the p-degree set defined as: for each vertex $v \in V(\zeta)$ the p-degree of the vertex v is denoted by d_{p_v} and defined as the number of minimal or minimum dominating set of ζ which contains v. The first and second domination Zagreb indices and modified first Zagreb domination indices are defined as:

$$DZ_1(\zeta) = \sum_{v \in V(\zeta)} d_{p_v}^2, \tag{1}$$

$$DZ_2(\zeta) = \sum_{uv \in E(\zeta)} \left[d_{p_u} \cdot d_{p_v} \right], \tag{2}$$

$$DZ_1^*(\zeta) = \sum_{uv \in E(\zeta)} \left[d_{p_u} + d_{p_v} \right]. \tag{3}$$

The forgotten domination, hyper domination, and modified forgotten domination indices of graphs are defined as:

$$DF(\zeta) = \sum_{v \in V(\zeta)} d_{p_v}^3, \tag{4}$$

$$DH(\zeta) = \sum_{uv \in E(\zeta)} \left[d_{p_u} + d_{p_v} \right]^2, \tag{5}$$

$$DF^*(\zeta) = \sum_{uv \in E(\zeta)} \left[d_{p_u}^2 + d_{p_v}^2 \right]. \tag{6}$$

In the realm of science, algebraic polynomials [19], such as the Omega polynomial [20, 21], Padmakar-Ivan (PI) [22], Zhang-Zhang [23], matching [24-26], Tutte [27], Schultz [28], and notably Hosoya polynomials [29], serve as pivotal tools for deriving various topological indices. These polynomials, especially those based on distance, like the Wiener [30] and hyper-Wiener index [31], offer insights into molecular structures. The M-polynomial, introduced in 2015 [32], stands out for its capacity to elucidate degree-based graph invariants, as supported by studies [33-36]. QSPR analysis further enhances this understanding, enabling predictive modeling that correlates topological indices

with polysaccharide properties. Such models are instrumental in areas like drug development, materials science, and understanding molecular interactions [37-41].

As computational techniques advance, they hold the potential to reshape our comprehension of polysaccharides, paving the way for novel polysaccharide-based innovations [42]. This has inspired our endeavor to refine domination topological indices, as previously introduced by one of the authors [18], using innovative polynomial approaches. In this study, the new polynomials represent $\varphi_{\tilde{\Re}}$-polynomial and φ_{γ}-polynomial. We study the $\varphi_{\tilde{\Re}}$-polynomial and φ_{γ}-polynomial by using minimal dominating sets (*M.D.S.*) and minimum dominating sets (*m.d.*s.) concepts for amylose and blue starch-iodine complex. A graphic interpretation is provided in addition to the results. The $\varphi_{\tilde{\Re}}$-polynomial is defined as:

$$\varphi_{\tilde{\Re}}(\zeta,x,y)=\sum_{\delta_{\tilde{\Re}}\le i\le j\le\Delta_{\tilde{\Re}}} d_{\tilde{\Re}}\ m_{(i,,j)}\ x^i y^j. \tag{7}$$

Where $d_{\tilde{\Re}}m_{(i,,j)}(\zeta)=\left|\left\{e=uv: d_{\tilde{\Re}_u}=i, d_{\tilde{\Re}_v}=j\right\}\right|$. The minimum and maximum domination degree of ζ are denoted by $\delta_{\tilde{\Re}}(\zeta)=\delta_{\tilde{\Re}}$ and $\Delta_{\tilde{\Re}}(\zeta)=\Delta_{\tilde{\Re}}$ respectively, where $\delta_{\tilde{\Re}}=min\{d_{\tilde{\Re}_v}: v\in V(\zeta)\}$ and $\Delta_{\tilde{\Re}}=max\{d_{\tilde{\Re}_v}: v\in V(\zeta)\}$. For each vertex $v\in V(\zeta)$, the domination value of v is defined as $d_{\gamma_v}=|\{S\subseteq V(\zeta): S \text{ is a } m.d.s. \text{ and } v\in S\}|$. The minimum and maximum domination value of a graph ζ by $\delta_{\gamma}(\zeta)=\delta_{\gamma}=min\{d_{\gamma_v}: v\in V(\zeta)\}$ and $\Delta_{\gamma}(\zeta)=\Delta_{\gamma}=max\{d_{\gamma_v}: v\in V(\zeta)\}$ respectively. The φ_{γ}-polynomial is defined as:

$$\varphi_{\gamma}(\zeta,x,y)=\sum_{\delta_{\gamma}\le i\le j\le\Delta_{\gamma}} d_{\gamma}\ m_{(i,,j)}x^i y^j. \tag{8}$$

Where $d_{\gamma}m_{(i,,j)}(\zeta)=\left|\left\{e=uv: d_{\gamma_u}=i, d_{\gamma_v}=j\right\}\right|$. Hence, $\tilde{\Re}$-domination ($\tilde{\Re}$) and γ-domination (γ) indices defined on $E(\zeta)$, which can be written as $\tilde{\Re}(\zeta)=\sum_{uv\in E(\zeta)} f(d_{\tilde{\Re}_u}, d_{\tilde{\Re}_v})$ and $\gamma(\zeta)=\sum_{uv\in E(\zeta)} f(d_{\gamma_u}, d_{\gamma_v})$. Hence, we define the $\tilde{\Re}$-domination and γ-domination topological indices from $\varphi_{\tilde{\Re}}$-polynomial and φ_{γ}-polynomial as in Table 1.

Table 1. Calculating domination topological indices via new polynomials

($\tilde{\Re}$) indices	Derivation from $\varphi_{\tilde{\Re}}(\zeta)$	(γ) indices	Derivation from $\varphi_{\gamma}(\zeta)$
$\tilde{\Re}Z_1^*(\zeta)$	$(D_x+D_y)\varphi_{\tilde{\Re}}(\zeta)\|_{x=y=1}$	$\gamma Z_1^*(\zeta)$	$(D_x+D_y)\varphi_{\gamma}(\zeta)\|_{x=y=1}$
$\tilde{\Re}F^*(\zeta)$	$(D_x^2+D_v^2)\varphi_{\tilde{\Re}}(\zeta)\|_{x=y=1}$	$\gamma F^*(\zeta)$	$(D_x^2+D_y^2)\varphi_{\gamma}(\zeta)\|_{x=y=1}$
$\tilde{\Re}Z_2(\zeta)$	$(D_xD_y)\varphi_{\tilde{\Re}}(\zeta)\|_{x=y=1}$	$\gamma Z_2(\zeta)$	$(D_xD_y)\varphi_{\gamma}(\zeta)\|_{x=y=1}$
$\tilde{\Re}H(\zeta)$	$(D_x+D_y)^2\varphi_{\tilde{\Re}}(\zeta)\|_{x=y=1}$	$\gamma H(\zeta)$	$(D_x+D_y)^2\varphi_{\gamma}(\zeta)\|_{x=y=1}$

Where $D_x(f(x,y))=x\frac{\partial(f(x,y))}{\partial x}$ and $D_y(f(x,y))=y\frac{\partial(f(x,y))}{\partial y}$.

In this article, we obtain the domination topological indices of a graph ζ of amylose and blue starch-iodine compounds for n = 2 via $\varphi_{\tilde{\Re}}$-polynomial and φ_{γ}-polynomial. The two compounds in their chair and boat isomeric forms are investigated with advanced quantum calculations, *DFT/TPSSTPSS/cc-pVTZ* using the Gaussian 09 software package in Section 2. In Sections 3 and 4, the domination topological indices via $\varphi_{\tilde{\Re}}$-polynomial and φ_{γ}-polynomial for amylose and blue starch-iodine complex are computed.

Furthermore, in Section 5, quantitative structure-property/activity relationship (QSPR/QSAR) analysis for $\tilde{}$-domination topological indices was performed to assess the efficacy of the calculated topological indices against the physicochemical properties of these polysaccharides amylose along with nicotine, aspirin, chloroquine, hydroxychloroquine, and anthraquinone. According to the results, the topological indices under study exhibit strong correlations with physicochemical properties.

2. Density functional theory (DFT) part

Starch binds cells with glucopyranose alpha bonds, which are glycosidic molecules formed from glucose. It consists of amylose and amylopectin. Glucose molecules assemble linearly into amylose. Amylose can't be dissolved in water. By breaking the glycosidic bonds (alpha bonds), it can be digested. Amounting to about 20 to 30 percent of starch, it is one of two components. As a result of its tight spiral structure, amylose is not digested as readily as other starch molecules, so it qualifies as a resistant starch [3]. Cycle degradants such as cyclodextrins form the bulk of amylose. Enzymatically, they form a circular path that is representative of an amylose helix imploding into single turns. A cyclodextrin dimer is stacked in front of all these complexes, generating large cylinders which, in their global structure, are similar to amylose helixes. A particularly interesting one is (trimesic acid $H_2O)_{10}HI_5$ with linear polyiodide chains. However, it is not possible to determine the exact form of the polyiodide chain from this structural model [4].

The monomers (\block building) of amylose and blue starch-iodine compounds are substituted cyclohexane rings. Cyclohexane and its derivatives are well known to exist in two main isomeric forms: boat and chair isomeric forms. In this work, one of density *TPSS* functional developed in the Truhlar group (*TPSSTPSS*) which include the meta-*GGA* part, was used to investigate the isomeric forms of the two investigated compounds [43]. *TPSS* functional are known to correctly describe hydrogen bonds, which needed to be clarified accurately in the boat and chair isomers.

The functional was combined with one of the basis sets developed by Dunning and coworkers, the triple-zeta *cc-pVTZ* [44]. In *cc-pVTZ* basis set, the '*cc-p*' stands for 'correlation-consistent polarized' and the '*V*' indicates they are valence-only basis sets. Frequency calculations were performed on each isomer at the same level of theory as required to validate the obtained structures as minima points in their potential energy surfaces; no negative (imaginary) frequency obtained. Calculations were performed on the Gaussian 09 suite program [45]. Molecular visualizations were performed using the GaussView program (version 5.0.8) [46].

Our results indicate that the blue starch-iodine compound is more stable than amylose in their two isomeric conformations. Since the electronic energies of the chair and boat forms of the blue starch-iodine compound are -690.83 and -690.896 Hartree, respectively, higher by not less than 3.38 Hartree than the corresponding ones of amylose.

Like the unsubstituted cyclohexane, the chair forms of amylose and blue starch-iodine are more stable than their boat forms since the chair form has a negligible ring strain. On the other hand, the boat forms are less stable for two reasons: (i) some eclipsed C-C bonds suffer from torsional strain, and (ii) some hydrogen atoms suffer from steric strain due to Van der Waals strain. From our calculations, the chair form of amylose is more stable than its boat form by 0.015 eV, while the chair form of blue starch-iodine is more stable than its boat form by 0.061 eV. Therefore, among the four investigated conformations, the chair form blue starch-iodine compound is the most stable conformer, and the boat form of amylose is the least stable conformation, see Figure 1.

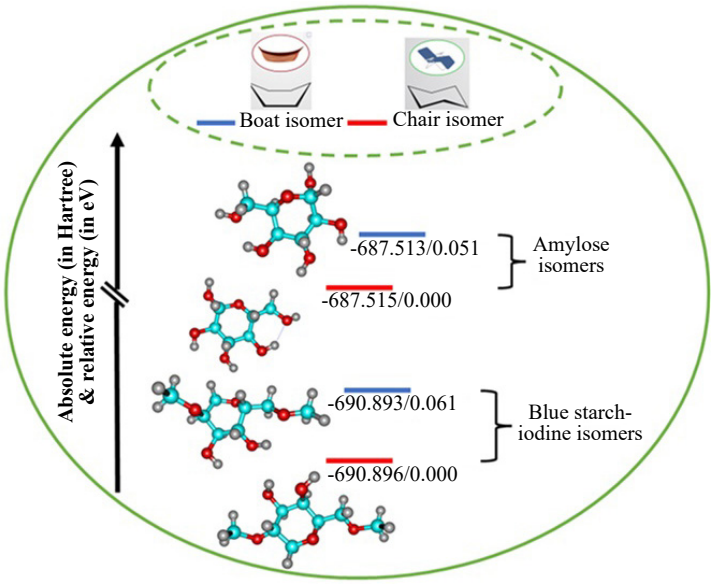

Figure 1. Energy diagram of chair and boat isomers of the two investigated compounds calculated by *DFT/TPSSTPSS/cc-pVTZ*

Table 2 lists some of the quantum chemical parameters (QCPs) of the two isomers for each compound. Such parameters are used to quantify the reactivity of each isomer. The energy gap, which is defined as the difference in energy between the highest occupied molecular orbital (*HOMO*) and the lowest unoccupied molecular orbital, measures the reactivity/stability of a conformation. The energy gap (ΔE_{gap}) of chair forms of the two investigated compounds is lower than that of their boat forms by not less than 0.7 eV and not more than 1.9 eV, thus, it is expected that the chair forms will be more reactive than their boat forms.

In addition, both the chair and boat forms of amylose are more reactive than those of blue starch-iodine, since the ΔE_{gap} value of the chair form is lower than that of blue starch-iodine by a significant amount, 1.4 eV, and the ΔE_{gap} value of the boat form is lower than that of blue starch-iodine by a less significant amount, 0.1 eV. This result is consistent with the stability order of amylose's and blue starch-iodine's isomers. In other words, the least stable isomers of amylose are more reactive than the most stable isomers of blue starch-iodine, see Figure 1. Other QCPs were calculated following Koopman's theory [47], and tabulated in Table 2. By using the following equations, we found the required values:

1. Energy gap, $\Delta E_{gap} = E_{LUMO} - E_{HOMO}$
2. Ionization energy, $I = -E_{HOMO}$.
3. Global hardness, $h = \frac{(I - E)}{2}$.
4. Electron affinity, $E = -E_{LUMO}$
5. Global softness, $s = \frac{1}{h}(/\mathrm{eV}^{-1})$.
6. Global electronegativity, $\chi = -\frac{(I + E)}{2}$.
7. Global electrophilicity, $\omega = \frac{(I + E)^2}{8(I + E)^2}$.
8. Chemical potential, $\mu = -\chi$.
9. Global nucleophilicity, $\epsilon = \frac{1}{\omega}$.

Table 2. QCPs (in eV, unless specified) of chair and boat isomers of the two investigated compounds

QCPs	Chair-amylose	Boat-amylose	Chair-starch-iodine	Boat-starch-iodine
HOMO energy, E_{HOMO}	-6.070	-5.961	-5.384	-5.523
LUMO energy, E_{LUMO}	-2.193	-0.150	-0.115	0.419
Energy gap	3.877	5.811	5.269	5.941
Ionization energy	6.070	5.961	5.384	5.5223
Electron affinity	2.193	0.150	0.115	-0.419
Global hardness	1.938	2.905	2.635	2.971
Global softness	0.516	0.344	0.380	0.337
Global electronegativity	4.132	3.056	2.750	2.552
Chemical potential	-4.132	-3.056	-2.750	-2.552
Global electrophilicity	4.403	1.607	1.435	1.096
Global nucleophilicity	0.227	0.622	0.697	0.912

3. Result for amylose

In this section, we will compute the domination topological indices $\varphi_{\tilde{\mathfrak{R}}}$-polynomial in Equation 7 and φ_{γ}-polynomial in Equation 8 for amylose. In Figure 2, the molecular structure of amylose is displayed and Figure 3, for its unit graph and the graph model corresponding to amylose for $n = 2$, where n is the number of units.

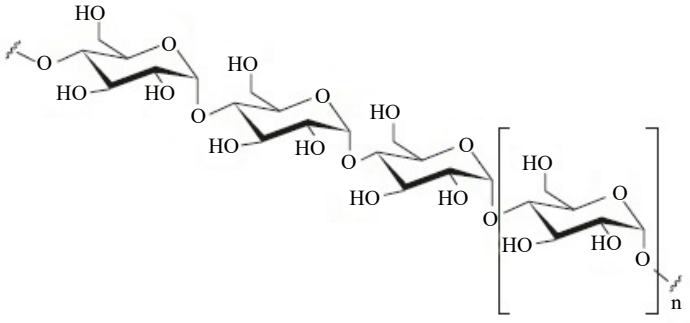

Figure 2. Molecular structure of amylose

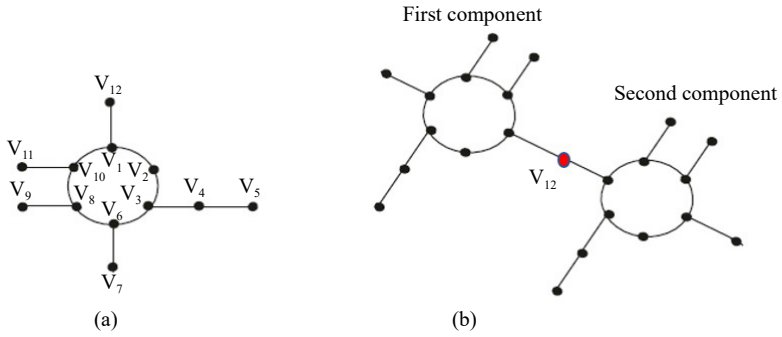

Figure 3. (a) Graph of amylose for $n = 1$; (b) graph of amylose for $n = 2$

Theorem 3.1. The total number of *M.D.S.* in the molecular graph ζ of amylose is 2544.

Proof. Let ζ be the molecular graph of amylose, we divide ζ into two components, and we compute the number of the *M.D.S.* of each component. First, we evaluate the number of the *M.D.S.* when $n = 1$. We can see that the *M.D.S.* when $n = 1$ are the following sets:

$$D_1 = \{v_2, v_8, v_{11}, v_{12}, v_4, v_7\}, \quad D_2 = \{v_2, v_8, v_{11}, v_{12}, v_5, v_7\}$$
$$D_3 = \{v_2, v_8, v_{11}, v_{12}, v_4, v_6\}, \quad D_4 = \{v_2, v_8, v_{11}, v_{12}, v_5, v_6\} \qquad (G1)$$

$$D_5 = \{v_8, v_{11}, v_1, v_4, v_7\}, \quad D_6 = \{v_2, v_8, v_{11}, v_1, v_5, v_7\}$$
$$D_7 = \{v_8, v_{11}, v_1, v_4, v_6\}, \quad D_8 = \{v_8, v_{11}, v_1, v_5, v_6\} \qquad (G2)$$

$$D_9 = \{v_2, v_8, v_{10}, v_{12}, v_4, v_7\}, \quad D_{10} = \{v_2, v_8, v_{10}, v_{12}, v_5, v_7\}$$
$$D_{11} = \{v_2, v_8, v_{10}, v_{12}, v_4, v_6\}, \quad D_{12} = \{v_2, v_8, v_{10}, v_{12}, v_5, v_6\} \qquad (G3)$$

$$D_{13} = \{v_8, v_{10}, v_1, v_4, v_7\}, \quad D_{14} = \{v_2, v_8, v_{10}, v_1, v_5, v_7\}$$
$$D_{15} = \{v_8, v_{10}, v_1, v_4, v_6\}, \quad D_{16} = \{v_8, v_{10}, v_1, v_5, v_6\} \qquad (G4)$$

$$D_{17} = \{v_2, v_9, v_{11}, v_{12}, v_4, v_7\}, \quad D_{18} = \{v_2, v_9, v_{11}, v_{12}, v_5, v_7\}$$
$$D_{19} = \{v_2, v_9, v_{11}, v_{12}, v_4, v_6\}, \quad D_{20} = \{v_2, v_9, v_{11}, v_{12}, v_5, v_6\} \qquad (G5)$$

$$D_{21} = \{v_9, v_{11}, v_1, v_4, v_7\}, \quad D_{22} = \{v_2, v_9, v_{11}, v_1, v_5, v_7\}$$
$$D_{23} = \{v_9, v_{11}, v_1, v_4, v_6\}, \quad D_{24} = \{v_9, v_{11}, v_1, v_5, v_6\} \qquad (G6)$$

$$D_{25} = \{v_2, v_9, v_{10}, v_{12}, v_4, v_7\}, \quad D_{26} = \{v_2, v_9, v_{10}, v_{12}, v_5, v_7\}$$
$$D_{27} = \{v_2, v_9, v_{10}, v_{12}, v_4, v_6\}, \quad D_{28} = \{v_2, v_9, v_{10}, v_{12}, v_5, v_6\} \qquad (G7)$$

$$D_{29} = \{v_9, v_{10}, v_1, v_4, v_7\}, \quad D_{30} = \{v_2, v_9, v_{10}, v_1, v_5, v_7\}$$
$$D_{31} = \{v_9, v_{10}, v_1, v_4, v_6\}, \quad D_{32} = \{v_9, v_{10}, v_1, v_5, v_6\} \qquad (G8)$$

$$D_{33} = \{v_3, v_8, v_{11}, v_{12}, v_4, v_7\}, \quad D_{34} = \{v_3, v_8, v_{11}, v_{12}, v_5, v_7\}$$
$$D_{35} = \{v_3, v_8, v_{11}, v_{12}, v_4, v_6\}, \quad D_{36} = \{v_3, v_8, v_{11}, v_{12}, v_5, v_6\} \qquad (G9)$$

$$D_{37} = \{v_3, v_8, v_{11}, v_1, v_5, v_7\} \qquad (G10)$$

$$D_{38} = \{v_3, v_8, v_{10}, v_{12}, v_4, v_7\}, \quad D_{39} = \{v_3, v_8, v_{10}, v_{12}, v_5, v_7\}$$
$$D_{40} = \{v_3, v_8, v_{10}, v_{12}, v_4, v_6\}, \quad D_{41} = \{v_3, v_8, v_{10}, v_{12}, v_5, v_6\} \qquad (G11)$$

$$D_{42} = \{v_3, v_8, v_{10}, v_1, v_5, v_7\} \qquad (G12)$$

$$D_{43} = \{v_3, v_9, v_{11}, v_{12}, v_4, v_7\}, \quad D_{44} = \{v_3, v_9, v_{11}, v_{12}, v_5, v_7\}$$
$$D_{45} = \{v_3, v_9, v_{11}, v_{12}, v_4, v_6\}, \quad D_{46} = \{v_3, v_9, v_{11}, v_{12}, v_5, v_6\} \qquad (G13)$$

$$D_{47} = \{v_3, v_9, v_{11}, v_1, v_5, v_7\} \qquad (G14)$$

$$D_{48} = \{v_3, v_9, v_{10}, v_{12}, v_4, v_7\}, \quad D_{49} = \{v_3, v_9, v_{10}, v_{12}, v_5, v_7\}$$
$$D_{50} = \{v_3, v_9, v_{10}, v_{12}, v_4, v_6\}, \quad D_{51} = \{v_3, v_9, v_{10}, v_{12}, v_5, v_6\} \qquad (G15)$$

$$D_{52} = \{v_3, v_9, v_{10}, v_1, v_5, v_7\} \qquad (G16)$$

Similarly, there are 52 *M.D.S.* for the second component. Now we add every *M.D.S.* in the first component to all *M.D.S.* in the second component. We obtain (4 × 52) = 208 *M.D.S.* when we add the first four *M.D.S.* in $G1$ of the first component to all dominating sets of the second component. Keeping in mind the minimalist condition, we obtain (3 × 38) + (1 × 58) = 172 when we add the *M.D.S.* of $G2$ to all dominating sets in the second component. Hence,

we notice the similarity of the groups $G1 \approx G3 \approx G5 \approx G7 \approx G9 \approx G11 \approx G13 \approx G15$ when we continue to add the *M.D.S.* of the first component to all *M.D.S.* in the second component we get the total number of *M.D.S.* for $n = 2$ is:

$$\overbrace{(4\times 52)}^{G1\times \text{all } M.D.S. \text{ of the second component}} + \overbrace{(3\times 38)+(1\times 58)}^{G2\times \text{all } M.D.S. \text{ of the second component}} + \overbrace{(4\times 52)}^{G3\times \text{all } M.D.S. \text{ of the second component}} + \overbrace{(3\times 38)+(1\times 58)}^{G4\times \text{all } M.D.S. \text{ of the second component}} +$$
$$\overbrace{(4\times 52)}^{G5\times \text{all } M.D.S. \text{ of the second component}} + \overbrace{(3\times 38)+(1\times 58)}^{G6\times \text{all } M.D.S. \text{ of the second component}} + \overbrace{(4\times 52)}^{G7\times \text{all } M.D.S. \text{ of the second component}} + \overbrace{(3\times 38)+(1\times 58)}^{G8\times \text{all } M.D.S. \text{ of the second component}} +$$
$$\overbrace{(4\times 52)}^{G9\times \text{all } M.D.S. \text{ of the second component}} + \overbrace{(1\times 38)}^{G10\times \text{all } M.D.S. \text{ of the second component}} + \overbrace{(4\times 52)}^{G11\times \text{all } M.D.S. \text{ of the second component}} + \overbrace{(1\times 58)}^{G12\times \text{all } M.D.S. \text{ of the second component}} +$$
$$\overbrace{(4\times 52)}^{G13\times \text{all } M.D.S. \text{ of the second component}} + \overbrace{(1\times 38)}^{G14\times \text{all } M.D.S. \text{ of the second component}} + \overbrace{(4\times 52)}^{G15\times \text{all } M.D.S. \text{ of the second component}} + \overbrace{(1\times 58)}^{G16\times \text{all } M.D.S. \text{ of the second component}}$$
$$= 2544.$$

Hence, the result.

We have 23 vertices in total in the molecular graph of amylose when $n = 2$. In order to compute the domination degree $d_{\tilde{\mathfrak{R}}_{v_i}}$ of each vertex v_i ($i = 1, \ldots, 23$) in this molecular graph, we have to count the number of dominating sets that consist of this vertex. For example, to compute the domination degree of v_1, we note that v_1 lies in the groups $G2$, $G4$, $G6$, $G8$, $G10$, $G12$, and $G14$. Now, when we add each *M.D.S.* of $G1$ of the first component to all *M.D.S.* in the second component, we get $(3 \times 38) + (1 \times 58)$ *M.D.S.* and v_1 is in $(3 \times 38) + 22 = 136$, which similar to the groups $G4$, $G6$, and $G8$. For $G10$ and $G14$, we get 38 *M.D.S.*, which are containing v_1. For $G12$ and $G16$, we obtain 22 *M.D.S.* Hence,

$$d_{\tilde{\mathfrak{R}}_{v1}} = \overbrace{(3\times 38)+22}^{G2\times \text{all } M.D.S. \text{ of second component}} + \overbrace{(3\times 38)+22}^{G4\times \text{all } M.D.S. \text{ of second component}} + \overbrace{(3\times 38)+22}^{G6\times \text{all } M.D.S. \text{ of second component}} + \overbrace{(3\times 38)+22}^{G8\times \text{all } M.D.S. \text{ of second component}} +$$
$$\overbrace{\widetilde{38}}^{G10\times \text{all } M.D.S. \text{ of second component}} + \overbrace{\widetilde{22}}^{G12\times \text{all } M.D.S. \text{ of second component}} + \overbrace{\widetilde{38}}^{G14\times \text{all } M.D.S. \text{ of second component}} + \overbrace{\widetilde{22}}^{G16\times \text{all } M.D.S. \text{ of second component}}$$
$$= (4\times 136)+2(38)+2(22) = 664.$$

Similar calculations for the other 22 vertices lead us to the following Tables 3 and 4.

Table 3. $\tilde{\mathfrak{R}}$-domination degrees of all vertices of the molecular graph of amylose

$d_{\tilde{\mathfrak{R}}_{v_i}}$	664	1064	1024	1136	1408	1120	1252	1292	1104
Number of vertices	2	2	2	2	4	4	2	2	1

Table 4. Edge partition based on the $\tilde{\mathfrak{R}}$-domination degree of the end vertices of each edge

(i,j) $d_{\tilde{\mathfrak{R}}_v} m_{(i,j)}$	(664, 1064) 1	(664, 1024) 1	(664, 1104) 2	(664, 1120) 1
(i,j) $d_{\tilde{\mathfrak{R}}_v} m_{(i,j)}$	(664, 1292) 1	(1024, 1064) 2	(1024, 1136) 2	(1136, 1408) 2
(i,j) $d_{\tilde{\mathfrak{R}}_v} m_{(i,j)}$	(1024, 1136) 1	(1064, 1136) 1	(1136, 1408) 2	(1136, 1292) 1
(i,j) $d_{\tilde{\mathfrak{R}}_v} m_{(i,j)}$	(1120, 1136) 1	(1120, 1292) 2	(1120, 1120) 2	(1252, 1292) 2

Theorem 3.2. If ζ is the molecular graph of amylose, then

1. $$\varphi_{\tilde{\Re}}(\zeta,x,y)=x^{664}\left[y^{1064}+y^{1024}+2y^{1104}+y^{1120}+y^{1292}\right]+x^{1024}\left[2y^{1064}+3y^{1136}\right]+x^{1136}\left[4y^{1408}+y^{1292}\right]$$
$$+y^{1136}\left[x^{1064}+x^{1120}\right]+x^{1120}\left[2y^{1292}+2y^{1120}\right]+2x^{1252}y^{1292}.$$
2. $\tilde{\Re}Z_1(\zeta)=31044928,\qquad \tilde{\Re}Z_2(\zeta)=29107712.$
$\tilde{\Re}Z_1^*(\zeta)=52800,\qquad \tilde{\Re}F(\zeta)=3.73750\times10^{10}.$
$\tilde{\Re}H(\zeta)=118138880,\qquad \tilde{\Re}F^*(\zeta)=59923456.$

Proof.

1. Let $d_{\tilde{\Re}}m_{(i,,j)}(\zeta)=\left|\left\{e=uv:d_{\tilde{\Re}_u}=i,d_{\tilde{\Re}_v}=j\right\}\right|$. The edge set of ζ can be divided into 16 partitions based on the domination degree of end vertices of each edge as given as in Table 3, then

$$\begin{aligned}\varphi_{\tilde{\Re}}(\zeta,x,y)&=\sum_{\delta_{\tilde{\Re}}\le i\le j\le\Delta_{\tilde{\Re}}} d_{\tilde{\Re}}\ m_{(i,,j)}\ x^iy^j\\
&=x^{664}y^{1064}+x^{664}y^{1024}+2x^{664}y^{1104}+x^{664}y^{1120}+x^{664}y^{1292}+2x^{1024}y^{1064}+2x^{1024}y^{1136}+2x^{1136}y^{1408}\\
&+x^{1024}y^{1136}+x^{1064}y^{1136}+2x^{1136}y^{1408}+x^{1136}y^{1292}+x^{1120}y^{1136}+2x^{1120}y^{1292}+2x^{1120}y^{1120}+2x^{1252}y^{1292}\\
&=x^{664}\left[y^{1064}+y^{1024}+2y^{1104}+y^{1120}+y^{1292}\right]+x^{1024}\left[2y^{1064}+3y^{1136}\right]+x^{1136}\left[4y^{1408}+y^{1292}\right]\\
&+x^{1136}\left[4y^{1408}+y^{1292}\right]+y^{1136}\left[x^{1064}+x^{1120}\right]+x^{1120}\left[2y^{1292}+2y^{1120}\right]+2x^{1252}y^{1292}.\end{aligned}$$

2. Now we compute the following to find the $\tilde{\Re}$-domination topological indices

$$\begin{aligned}D_x\left[\varphi_{\tilde{\Re}}(\zeta,x,y)\right]&=664x^{664}\left[y^{1064}+y^{1024}+2y^{1104}+y^{1120}+y^{1292}\right]+1024x^{1024}\left[2y^{1064}+3y^{1136}\right]\\
&+1136x^{1136}\left[4y^{1408}+y^{1292}\right]+y^{1136}\left[1064x^{1064}+1120x^{1120}\right]+1120x^{1120}\left[2y^{1292}+2y^{1120}\right]\\
&+2504x^{1252}y^{1292},\end{aligned}$$

which implies that

$$\begin{aligned}D_x^2\left[\varphi_{\tilde{\Re}}(\zeta,x,y)\right]&=440896x^{664}\left[y^{1064}+y^{1024}+2y^{1104}+y^{1120}+y^{1292}\right]+1048576x^{1024}\left[2y^{1064}+3y^{1136}\right]\\
&+1290496x^{1136}\left[4y^{1408}+y^{1292}\right]+y^{1136}\left[1132096x^{1064}+1254400x^{1120}\right]\\
&+1254400x^{1120}\left[2y^{1292}+2y^{1120}\right]+3135008x^{1252}y^{1292},\end{aligned}$$

$$\begin{aligned}D_y\left[\varphi_{\tilde{\Re}}(\zeta,x,y)\right]&=x^{664}\left[1064y^{1064}+1024y^{1024}+2208y^{1104}+1120y^{1120}+1292y^{1292}\right]\\
&+x^{1024}\left[2128y^{1064}+3408y^{1136}\right]+x^{1136}\left[5632y^{1408}+1292y^{1292}\right]+1136y^{1136}\left[x^{1064}+x^{1120}\right]\\
&+x^{1120}\left[2584y^{1292}+2240y^{1120}\right]+2584x^{1252}y^{1292},\end{aligned}$$

which implies that

$$\begin{aligned}D_y^2\left[\varphi_{\tilde{\Re}}(\zeta,x,y)\right]&=x^{664}\left[1132096y^{1064}+1048576y^{1024}+2437632y^{1104}+1254400y^{1120}+1669264y^{1292}\right]\\
&+x^{1024}\left[2264192y^{1064}+3871488y^{1136}\right]+x^{1136}\left[7924856y^{1408}+1669264y^{1292}\right]\\
&+1290496y^{1136}\left[x^{1064}+x^{1120}\right]+x^{1120}\left[3338528y^{1292}+2508800y^{1120}\right]+3338528x^{1252}y^{1292}\end{aligned}$$

and

$$D_xD_y\left[\varphi_{\tilde{\Re}}(\zeta,x,y)\right]=664x^{664}\left[1064y^{1064}+1024y^{1024}+2208y^{1104}+1120y^{1120}+1292y^{1292}\right]$$
$$+1024x^{1024}\left[2128y^{1064}+3408y^{1136}\right]+1136x^{1136}\left[5632y^{1408}+1292y^{1292}\right]$$
$$+1136y^{1136}\left[1064x^{1064}+1120x^{1120}\right]+1120x^{1120}\left[2584y^{1292}+2240y^{1120}\right]$$
$$+3235168x^{1252}y^{1292}.$$

Now,

$$\tilde{\Re}Z_1^*(\zeta)=\left(D_x+D_y\right)\left[\varphi_{\tilde{\Re}}(\zeta,x,y)\right]|_{x=y=1}$$
$$=x^{664}\begin{bmatrix}1728y^{1064}\\+1688y^{1024}\\+3536y^{1104}\\+1784y^{1120}\\+1956y^{1292}\end{bmatrix}+x^{1024}\begin{bmatrix}4176y^{1064}+\\6480y^{1136}\end{bmatrix}+x^{1136}\begin{bmatrix}10176y^{1408}+\\2428y^{1292}\end{bmatrix}+y^{1136}\begin{bmatrix}2200x^{1064}+\\2256x^{1120}\end{bmatrix}+x^{1120}\begin{bmatrix}4824y^{1292}+\\4480y^{1120}\end{bmatrix}$$
$$+5088x^{1252}y^{1292}\,|_{x=y=1}$$
$$=10692+10656+12604+4456+9304+5088=52800.$$

$$\tilde{\Re}Z_2(\zeta)=\left(D_xD_y\right)\left[\varphi_{\tilde{\Re}}(\zeta,x,y)\right]|_{x=y=1}$$
$$=664x^{664}\begin{bmatrix}1064y^{1064}+\\1024y^{1024}+\\2208y^{1104}+\\1120y^{1120}+\\1292y^{1292}\end{bmatrix}+1024x^{1024}\begin{bmatrix}2128y^{1064}+\\3408y^{1136}\end{bmatrix}+1136x^{1136}\begin{bmatrix}5632y^{1408}+\\1292y^{1292}\end{bmatrix}+1136y^{1136}\begin{bmatrix}1064x^{1064}+\\1120x^{1120}\end{bmatrix}$$
$$+1120x^{1120}\begin{bmatrix}2584y^{1292}+\\2240y^{1120}\end{bmatrix}+3235168x^{1252}y^{1292}\,|_{x=y=1}$$
$$=4454112+5668864+7865664+2481024+5402880+323516=29107712.$$

$$\tilde{\Re}F^*(\zeta)=\left(D_x^2+D_y^2\right)\left[\varphi_{\tilde{\Re}}(\zeta,x,y)\right]|_{x=y=1}$$
$$=x^{664}\begin{bmatrix}157992y^{1064}+\\1489472y^{1024}+\\3319424y^{1104}+\\1695296y^{1120}+\\2110160y^{1292}\end{bmatrix}+x^{1024}\begin{bmatrix}4361344y^{1064}+\\7017216y^{1136}\end{bmatrix}+x^{1136}\begin{bmatrix}13091840y^{1408}+\\2959760y^{1292}\end{bmatrix}+y^{1136}\begin{bmatrix}2422592x^{1064}+\\2544896x^{1120}\end{bmatrix}$$
$$+x^{1120}\begin{bmatrix}5847328y^{1292}+\\5017600y^{1120}\end{bmatrix}+6473536x^{1252}y^{1292}\,|_{x=y=1}$$
$$=10187344+11378560+16051600+4967488+10864928+6473536=59923456.$$

$$\tilde{\Re}H(\zeta)=\left(D_x^2+D_y^2+2D_xD_y\right)\left[\varphi_{\tilde{\Re}}\left(\zeta,x,y\right)\right]|_{x=y=1}$$

$$=x^{664}\begin{bmatrix}2985984y^{1064}+\\2849344y^{1024}+\\6251648y^{1104}+\\3182656y^{1120}+\\3825936y^{1242}\end{bmatrix}+x^{1024}\begin{bmatrix}8719488y^{1064}+\\13996800y^{1136}\end{bmatrix}+x^{1136}\begin{bmatrix}25887744y^{1408}+\\5895184y^{1242}\end{bmatrix}+y^{1136}\begin{bmatrix}4840000x^{1064}+\\5089536x^{1120}\end{bmatrix}$$

$$+x^{1120}\begin{bmatrix}11635488y^{1292}+\\10035200y^{1120}\end{bmatrix}+12943872x^{1252}y^{1292}\,|_{x=y=1}$$

$$=19095568+54499216+31600224+12943872=118138880.$$

$$\tilde{\Re}Z_1(\zeta)=\sum_{v\in V(\zeta)}d_{\tilde{\Re}}^2$$

$$=2\left(664\right)^2+4\left(1120\right)^2+2\left(1024\right)^2+4\left(1408\right)^2+2\left(1064\right)^2+2\left(1292\right)^2+2\left(1252\right)^2+\left(1104\right)^2$$

$$=31044928.$$

$$\tilde{\Re}F(\zeta)=\sum_{v\in V(\zeta)}d_{\tilde{\Re}}^3$$

$$=2\left(664\right)^3+4\left(1120\right)^3+2\left(1024\right)^3+4\left(1408\right)^3+2\left(1064\right)^3+2\left(1292\right)^3+2\left(1252\right)^3+\left(1104\right)^3$$

$$=3.73750\times10^{10}.$$

This completes the proof.

In the next theorem, we will give the *m.d.s*. of amylose.

Theorem 3.3. The total number of *m.d.s*. in the molecular graph ζ of amylose is 24.

Proof. Let ζ be the molecular graph of amylose, we have the following *m.d.s*. for the first component:

$$D_1=\{v_8,v_{11},v_1,v_4,v_7\},\ D_2=\{v_8,v_{11},v_1,v_4,v_6\},\ D_3=\{v_8,v_{11},v_1,v_5,v_6\}$$
$$D_4=\{v_8,v_{10},v_1,v_4,v_7\},\ D_5=\{v_8,v_{10},v_1,v_4,v_6\},\ D_6=\{v_8,v_{10},v_1,v_5,v_6\}$$
$$D_7=\{v_9,v_{11},v_1,v_4,v_7\},\ D_8=\{v_9,v_{11},v_1,v_4,v_6\},\ D_9=\{v_9,v_{11},v_1,v_5,v_6\}$$
$$D_{10}=\{v_9,v_{10},v_1,v_4,v_7\},\ D_{11}=\{v_9,v_{10},v_1,v_4,v_6\},\ D_{12}=\{v_9,v_{10},v_1,v_5,v_6\}.$$

For the second component, we have the following *m.d.s*.:

$$D_1^{'}=\{v_{14},v_{17},v_{18},v_{22},v_{12}\},\ D_2^{'}=\{v_{14},v_{17},v_{18},v_{22},v_{13}\},\ D_3^{'}=\{v_{14},v_{17},v_{18},v_{23},v_{13}\}$$
$$D_4^{'}=\{v_{14},v_{16},v_{18},v_{22},v_{12}\},\ D_5^{'}=\{v_{14},v_{16},v_{18},v_{22},v_{13}\},\ D_6^{'}=\{v_{14},v_{16},v_{18},v_{23},v_{13}\}$$
$$D_7^{'}=\{v_{15},v_{17},v_{18},v_{22},v_{12}\},\ D_8^{'}=\{v_{15},v_{17},v_{18},v_{22},v_{13}\},\ D_9^{'}=\{v_{15},v_{17},v_{18},v_{23},v_{13}\}$$
$$D_{10}^{'}=\{v_{15},v_{16},v_{18},v_{22},v_{12}\},\ D_{11}^{'}=\{v_{15},v_{16},v_{18},v_{22},v_{13}\},\ D_{12}^{'}=\{v_{15},v_{16},v_{18},v_{23},v_{13}\}.$$

In order to compute the *m.d.s*. for n = 2, we have combined the sets in the first component with all sets in the second component keeping in mind the minimum condition, we obtain the following dominating sets:

$$\overbrace{F_1=\{v_8,v_{11},v_1,v_4,v_7,v_{14},v_{17},v_{18},v_{22}\}}^{\text{from } D_1 \text{ and all } m.d.s. \text{ in the second component}},\ F_2=\{v_8,v_{11},v_1,v_4,v_7,v_{14},v_{16},v_{18},v_{22}\}$$

$$\overbrace{F_3=\{v_8,v_{11},v_1,v_4,v_6,v_{14},v_{17},v_{18},v_{22}\}}^{\text{from } D_2 \text{ and all } m.d.s. \text{ in the second component}},\ F_4=\{v_8,v_{11},v_1,v_4,v_6,v_{14},v_{16},v_{18},v_{22}\}$$

$$\overbrace{F_5=\{v_8,v_{11},v_1,v_5,v_6,v_{14},v_{17},v_{18},v_{22}\}}^{\text{from } D_3 \text{ and all } m.d.s. \text{ in the second component}},\ F_6=\{v_8,v_{11},v_1,v_5,v_6,v_{14},v_{16},v_{18},v_{22}\}$$

$$\overbrace{F_7=\{v_8,v_{10},v_1,v_4,v_7,v_{14},v_{17},v_{18},v_{22}\}}^{\text{from } D_4 \text{ and all } m.d.s. \text{ in the second component}},\ \overbrace{F_8=\{v_8,v_{10},v_1,v_4,v_7,v_{14},v_{16},v_{18},v_{22}\}}^{}$$

$$\overbrace{F_9=\{v_8,v_{10},v_1,v_4,v_6,v_{14},v_{17},v_{18},v_{22}\}}^{\text{from } D_5 \text{ and all } m.d.s. \text{ in the second component}},\ \overbrace{F_{10}=\{v_8,v_{10},v_1,v_4,v_6,v_{14},v_{16},v_{18},v_{22}\}}^{}$$

$$\overbrace{F_{11}=\{v_8,v_{10},v_1,v_5,v_6,v_{14},v_{17},v_{18},v_{22}\}}^{\text{from } D_6 \text{ and all } m.d.s. \text{ in the second component}},\ \overbrace{F_{12}=\{v_8,v_{10},v_1,v_5,v_6,v_{14},v_{16},v_{18},v_{22}\}}^{}$$

$$\overbrace{F_{13}=\{v_9,v_{11},v_1,v_4,v_7,v_{14},v_{17},v_{18},v_{22}\}}^{\text{from } D_7 \text{ and all } m.d.s. \text{ in the second component}},\ \overbrace{F_{14}=\{v_9,v_{11},v_1,v_4,v_7,v_{14},v_{16},v_{18},v_{22}\}}^{}$$

$$\overbrace{F_{15}=\{v_9,v_{11},v_1,v_4,v_6,v_{14},v_{17},v_{18},v_{22}\}}^{\text{from } D_8 \text{ and all } m.d.s. \text{ in the second component}},\ \overbrace{F_{16}=\{v_9,v_{11},v_1,v_4,v_7,v_{14},v_{16},v_{18},v_{22}\}}^{}$$

$$\overbrace{F_{17}=\{v_9,v_{11},v_1,v_5,v_6,v_{14},v_{17},v_{18},v_{22}\}}^{\text{from } D_9 \text{ and all } m.d.s. \text{ in the second component}},\ \overbrace{F_{18}=\{v_9,v_{11},v_1,v_5,v_6,v_{14},v_{16},v_{18},v_{22}\}}^{}$$

$$\overbrace{F_{19}=\{v_9,v_{10},v_1,v_4,v_7,v_{14},v_{17},v_{18},v_{22}\}}^{\text{from } D_{10} \text{ and all } m.d.s. \text{ in the second component}},\ \overbrace{F_{20}=\{v_9,v_{10},v_1,v_4,v_7,v_{14},v_{16},v_{18},v_{22}\}}^{}$$

$$\overbrace{F_{21}=\{v_9,v_{10},v_1,v_4,v_6,v_{14},v_{17},v_{18},v_{22}\}}^{\text{from } D_{11} \text{ and all } m.d.s. \text{ in the second component}},\ \overbrace{F_{22}=\{v_9,v_{10},v_1,v_4,v_6,v_{14},v_{16},v_{18},v_{22}\}}^{}$$

$$\overbrace{F_{23}=\{v_9,v_{10},v_1,v_5,v_6,v_{14},v_{17},v_{18},v_{22}\}}^{\text{from } D_{12} \text{ and all } m.d.s. \text{ in the second component}},\ \overbrace{F_{24}=\{v_9,v_{10},v_1,v_5,v_6,v_{14},v_{16},v_{18},v_{22}\}}^{}$$

Hence, we can conclude that we have 24 *m.d.s*. of amylose.
With some calculations, we obtain the following Tables 5 and 6.

Table 5. γ-domination degrees of all vertices of the molecular graph of amylose

d_γ	0	8	12	16	18
Number of vertices	9	2	6	2	4

Table 6. Edge partition based on the γ-domination degree of the end vertices of each edge

(i,j)	(0,0)	(0,16)	(0,24)	(8,16)	(12,12)	(12,16)	(12,24)
$d_\gamma m_{(i,j)}$	4	2	8	2	4	1	3

In the next Theorem 3.4, we compute the γ-domination topological indices via γ-polynomial.

Theorem 3.4. If ζ is the molecular graph of amylose, then

1. $\varphi_\gamma(\zeta,x,y)=4+2y^{16}+8y^{24}+2x^8y^{16}+4x^{12}y^{12}+x^{12}y^{16}+3x^{12}y^{24}$.
2. $\gamma Z_1(\zeta)=3808, \quad \gamma Z_2(\zeta)=1888.$
   $\gamma Z_1^*(\zeta)=504, \quad \gamma F(\zeta)=74880.$
   $\gamma H(\zeta)=13248, \quad \gamma F^*(\zeta)=9472.$

Proof.

1. Let $d_\gamma m_{(i,,j)}(\zeta)=\left|\{e=uv: d_\gamma=i, d_\gamma=j\}\right|$. The edge set of ζ can be divided into 7 partitions based on the γ-domination degree of end vertices of each edge as given in Table 6, then

$$\begin{aligned}\varphi_\gamma(\zeta,x,y) &= \sum_{\delta_\gamma \le i \le j \le \Delta_\gamma} d_\gamma m_{(i,,j)} x^i y^j \\ &= 4x^0y^0 + 2x^0y^{16} + 8x^0y^{24} + 2x^8y^{16} + 4x^{12}y^{12} + 3x^{12}y^{24} \\ &= 4 + 2y^{16} + 8y^{24} + 2x^8y^{16} + 4x^{12}y^{12} + x^{12}y^{16} + 3x^{12}y^{24}.\end{aligned}$$

2. Now, we compute the following to find the γ-domination topological indices

$$D_x\left[\varphi_\gamma(\zeta,x,y)\right] = 16x^8y^{16} + 48x^{12}y^{12} + 12x^{12}y^{16} + 36x^{12}y^{24},$$

which implies that

$$\begin{aligned}D_x^2\left[\varphi_\gamma(\zeta,x,y)\right] &= 128x^8y^{16} + 576x^{12}y^{12} + 144x^{12}y^{16} + 432x^{12}y^{24} \\ D_y\left[\varphi_\gamma(\zeta,x,y)\right] &= 16x^8y^{16} + 48x^{12}y^{12} + 12x^{12}y^{16} + 36x^{12}y^{24},\end{aligned}$$

which implies that

$$D_y^2\left[\varphi_\gamma(\zeta,x,y)\right] = 512y^{16} + 4608y^{24} + 512x^8y^{16} + 576x^{12}y^{12} + 256x^{12}y^{16} + 1728x^{12}y^{24}$$

and

$$D_xD_y\left[\varphi_\gamma(\zeta,x,y)\right] = 256x^8y^{16} + 576x^{12}y^{12} + 192x^{12}y^{16} + 864x^{12}y^{24}.$$

Now,

$$\begin{aligned}\gamma Z_1^*(\zeta) &= \left(D_x + D_y\right)\left[\varphi_\gamma(\zeta,x,y)\right]|_{x=y=1} \\ &= 32y^{16} + 192y^{24} + 48x^8y^{16} + 96x^{12}y^{12} + 28x^{12}y^{16} + 108x^{12}y^{24}\,|_{x=y=1} \\ &= 504. \\ \gamma Z_2(\zeta) &= \left(D_xD_y\right)\left[\varphi_\gamma(\zeta,x,y)\right]|_{x=y=1} \\ &= 256x^8y^{16} + 576x^{12}y^{12} + 192x^{12}y^{16} + 864x^{12}y^{24}\,|_{x=y=1} \\ &= 1888. \\ \gamma F^*(\zeta) &= \left(D_x^2 + D_y^2\right)\left[\varphi_\gamma(\zeta,x,y)\right]|_{x=y=1} \\ &= 512y^{16} + 4608x^8y^{16} + 1152x^{12}y^{12} + 400x^{12}y^{16} + 2160x^{12}y^{24}\,|_{x=y=1} \\ &= 9472. \\ \gamma H(\zeta) &= \left(D_x^2 + D_y^2 + 2D_xD_y\right)\left[\varphi_\gamma(\zeta,x,y)\right]|_{x=y=1} \\ &= 512y^{16} + 4608y^{24} + 1152x^8y^{16} + 2304x^{12}y^{12} + 784x^{12}y^{16} + 3888x^{12}y^{24}\,|_{x=y=1} \\ &= 13248. \\ \gamma Z_1(\zeta) &= \sum_{v\in V(\zeta)} d_\gamma^2 = 9(0)^2 + 2(8)^2 + 6(12)^2 + 2(16)^2 + 4(24)^2 = 3808. \\ \gamma F(\zeta) &= \sum_{v\in V(\zeta)} d_\gamma^3 = 9(0)^3 + 2(8)^3 + 6(12)^3 + 2(16)^3 + 4(24)^3 = 74880.\end{aligned}$$

This completes the proof.

In Figure 4, we present the 3D representation of $\varphi_{\mathfrak{R}}$-polynomial and φ_γ-polynomial of amylose.

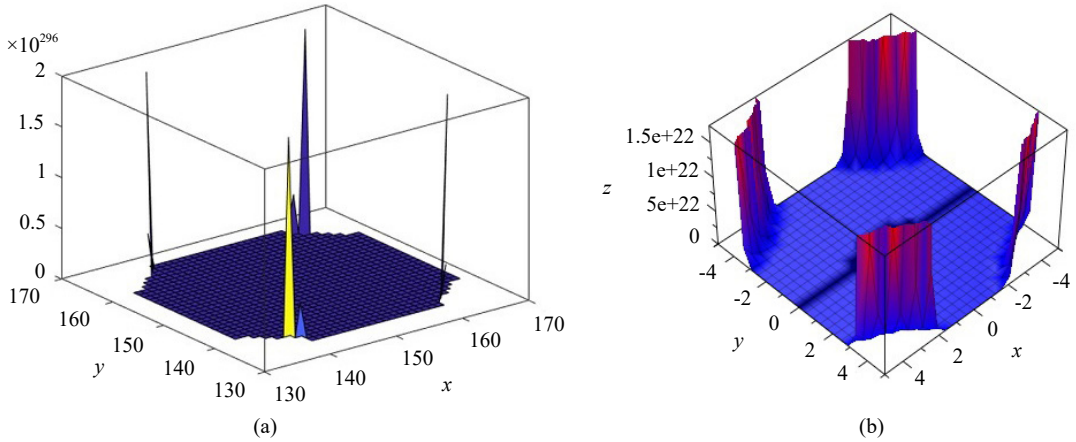

Figure 4. Plotting of (a) $\varphi_{\tilde{\mathfrak{R}}}$-polynomial; (b) φ_{γ}-polynomial of amylose

4. Results for blue starch-iodine complex

In this section, we will compute the domination topological indices via the $\tilde{\mathfrak{R}}$-polynomial in Equation 7, and the φ_{γ} -polynomial in Equation 8 for the blue starch-iodine complex. Figure 5 is the molecular structure of blue starch-iodine, and Figure 6 shows the unit graph and the graph model corresponding to blue starch-iodine for n = 2, where n is the number of units.

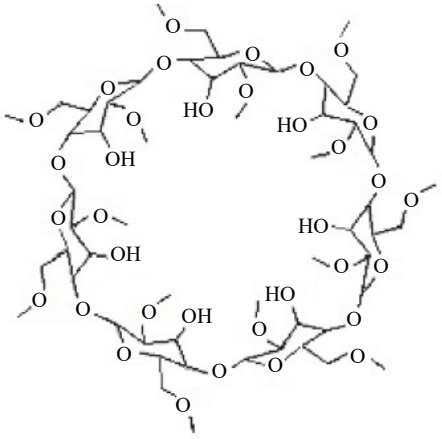

Figure 5. Molecular structure of blue starch-iodine

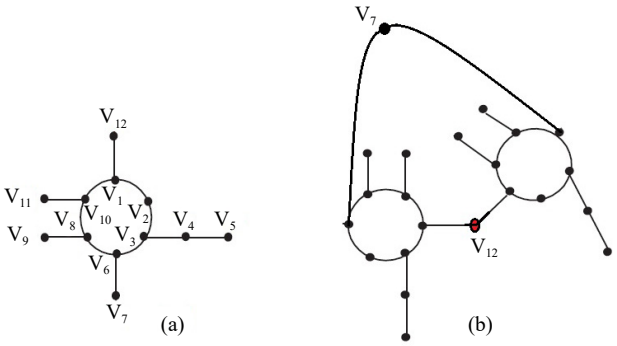

Figure 6. (a) Graph of blue starch-iodine for n = 1; (b) graph of blue starch-iodine for n = 2

Theorem 4.1. The total number of *M.D.S.* and *m.d.s.* in the molecular graph of blue starch-iodine for $n = 2$, is 1874 and 16, respectively.

Proof. Notice that in the two components of blue starch-iodine the *M.D.S.* is the same number of the *M.D.S.*s of amylose.

First, we compute the *M.D.S.* of the molecular graph of blue starch-iodine for $n = 2$

$$\overbrace{(2\times 44)+(2\times 29)}^{G1\times \text{all } M.D.S. \text{ of the second component}} + \overbrace{(3\times 33)+(26)}^{G2\times \text{all } M.D.S. \text{ of the second component}} + \overbrace{(2\times 44)+(2\times 29)}^{G3\times \text{all } M.D.S. \text{ of the second component}} + \overbrace{(3\times 33)+(26)}^{G4\times \text{all } M.D.S. \text{ of the second component}} +$$
$$\overbrace{(4\times 44)}^{G5\times \text{all } M.D.S. \text{ of the second component}} + \overbrace{(4\times 33)}^{G6\times \text{all } M.D.S. \text{ of the second component}} + \overbrace{(4\times 44)}^{G7\times \text{all } M.D.S. \text{ of the second component}} + \overbrace{(4\times 33)}^{G8\times \text{all } M.D.S. \text{ of the second component}} +$$
$$\overbrace{(2\times 44)+(2\times 29)}^{G9\times \text{all } M.D.S. \text{ of the second component}} + \overbrace{(33)}^{G10\times \text{all } M.D.S. \text{ of the second component}} + \overbrace{(2\times 44)+(2\times 29)}^{G11\times \text{all } M.D.S. \text{ of the second component}} + \overbrace{(33)}^{G12\times \text{all } M.D.S. \text{ of the second component}} +$$
$$\overbrace{(2\times 44)+(2\times 29)}^{G13\times \text{all } M.D.S. \text{ of the second component}} + \overbrace{(33)}^{G14\times \text{all } M.D.S. \text{ of the second component}} + \overbrace{(2\times 44)+(2\times 29)}^{G15\times \text{all } M.D.S. \text{ of the second component}} + \overbrace{(33)}^{G16\times \text{all } M.D.S. \text{ of the second component}}$$
$$=(6\times 146)+(2\times 125)+(2\times 176)+(2\times 132)+(4\times 33)$$
$$=1874.$$

Second, we compute the *m.d.s.* of the molecular graph of blue starch-iodine for $n = 2$; we follow the same steps of Theorem 3.3, keeping in mind the minimum condition, we conclude the following:

$$F_1' = \{v_8, v_{11}, v_1, v_4, v_7, v_{14}, v_{17}, v_{22}\},\ F_2' = \{v_8, v_{11}, v_1, v_4, v_7, v_{14}, v_{16}, v_{22}\},$$
$$F_3' = \{v_8, v_{11}, v_1, v_4, v_6, v_{14}, v_{16}, v_{22}\},\ F_4' = \{v_8, v_{11}, v_1, v_5, v_6, v_{14}, v_{16}, v_{22}\},$$
$$F_5' = \{v_8, v_{10}, v_1, v_4, v_7, v_{14}, v_{17}, v_{22}\},\ F_6' = \{v_8, v_{10}, v_1, v_4, v_7, v_{14}, v_{16}, v_{22}\},$$
$$F_7' = \{v_8, v_{10}, v_1, v_4, v_6, v_{14}, v_{16}, v_{22}\},\ F_8' = \{v_8, v_{10}, v_1, v_5, v_6, v_{14}, v_{16}, v_{22}\},$$
$$F_9' = \{v_9, v_{11}, v_1, v_4, v_7, v_{14}, v_{17}, v_{22}\},\ F_{10}' = \{v_9, v_{11}, v_1, v_4, v_7, v_{14}, v_{16}, v_{22}\},$$
$$F_{11}' = \{v_9, v_{11}, v_1, v_4, v_6, v_{14}, v_{16}, v_{22}\},\ F_{12}' = \{v_9, v_{11}, v_1, v_5, v_6, v_{14}, v_{16}, v_{22}\},$$
$$F_{13}' = \{v_9, v_{10}, v_1, v_4, v_7, v_{14}, v_{17}, v_{22}\},\ F_{14}' = \{v_9, v_{10}, v_1, v_4, v_7, v_{14}, v_{16}, v_{22}\},$$
$$F_{15}' = \{v_9, v_{10}, v_1, v_4, v_6, v_{14}, v_{16}, v_{22}\},\ F_{16}' = \{v_9, v_{10}, v_1, v_5, v_6, v_{14}, v_{16}, v_{22}\}.$$

Hence, we have 16 *m.d.s.*

With some calculations, we obtain the following Tables 7 to 10.

Table 7. The $\Re$-domination degrees of all vertices of the molecular graph of blue starch-iodine complex

$d_{\Re_v}$	770	774	716	864	1010	762	646	937	900	974
Number of vertices	1	2	2	2	2	2	2	4	2	2

Table 8. Edge partition based on the $\tilde{\Re}$-domination degree of the end vertices of each edge

(i,j)	(646,744)	(646,937)	(646,716)	(664,761)
$d_{\tilde{\Re}}\, m_{(i,j)}$	2	2	1	1
(i,j)	(716,762)	(716,846)	(716,774)	(762,774)
$d_{\tilde{\Re}}\, m_{(i,j)}$	2	2	1	1
(i,j)	(770,744) (864,1010)	(864,1010)	(774,900)	(900,937)
$d_{\tilde{\Re}}\, m_{(i,j)}$	2	2	2	2
(i,j)	(900,947)	(937,937)	/	/
$d_{\tilde{\Re}}\, m_{(i,j)}$	2	2	/	/

Table 9. The γ-domination degrees of all vertices of the molecular graph of blue starch-iodine complex

d_γ	0	4	8	12	16
Number of vertices	9	2	6	2	3

Table 10. Edge partition based on the γ-domination degree of the end vertices of each edge

(i,j)	(0,0)	(0,16)	(0,24)	(8,16)	(12,12)	(12,16)	(12,24)
$d_\gamma m_{(i,j)}$	4	2	8	2	4	1	3

In the next Theorem 4.2, we compute the $\tilde{\Re}$-domination topological indices via $\tilde{\Re}$-polynomial.

Theorem 4.2. If ζ is the molecular graph of blue starch-iodine complex, then

1. $$\varphi_{\tilde{\Re}}(\zeta,x,y) = x^{646}\left[2y^{744}+2y^{937}+y^{716}+y^{762}\right]+x^{716}\left[2y^{762}+2y^{864}+y^{774}\right]+y^{774}[x^{762}+2x^{770}]$$
$$+x^{900}[2y^{937}+2y^{974}]+2x^{864}y^{1010}+2x^{937}y^{937}+2x^{774}y^{900}.$$
2. $\tilde{\Re}Z_1(\zeta)=15928240,$ $\tilde{\Re}Z_2(\zeta)=16125222.$
$\tilde{\Re}Z_1^*(\zeta)=39212,$ $\tilde{\Re}F(\zeta)=1.39011263\times10^{10}.$
$\tilde{\Re}H(\zeta)=64847468,$ $\tilde{\Re}F^*(\zeta)=32597024.$

Proof. For (1), similar steps on proof of Theorem 3.2. For part (2), in order to find the $\tilde{\Re}$-domination topological indices, we need the following calculations

$$D_x\left[\varphi_{\tilde{\Re}}(\zeta,x,y)\right]=646x^{646}\left[2y^{744}+2y^{937}+y^{716}+y^{762}\right]+716x^{716}\left[2y^{762}+2y^{864}+y^{774}\right]$$
$$+y^{774}\left[762x^{762}+1540x^{770}\right]+900x^{900}\left[2y^{937}+2y^{974}\right]+17280x^{864}y^{1010}+1874x^{937}y^{937}$$
$$+1548x^{774}y^{900},$$

which implies that

$$D_x^2\left[\varphi_{\tilde{\mathfrak{R}}}(\zeta,x,y)\right]=417316x^{646}\left[2y^{744}+2y^{937}+y^{716}+y^{762}\right]+5126562x^{716}\left[2y^{762}+2y^{864}+y^{774}\right]$$
$$+y^{774}\left[580644x^{762}+1185800x^{770}\right]+810000x^{900}\left[2y^{937}+2y^{974}\right]+1492992x^{864}y^{1010}$$
$$+1755938x^{937}y^{937}+1198152x^{774}y^{900},$$

$$D_y\left[\varphi_{\tilde{\mathfrak{R}}}(\zeta,x,y)\right]=x^{646}\left[1488y^{744}+1874y^{937}+716y^{716}+762y^{762}\right]+716x^{716}\left[1524y^{762}+1728y^{864}+774y^{774}\right]$$
$$+774y^{774}\left[x^{762}+2x^{770}\right]+900x^{900}\left[1874y^{937}+1948y^{974}\right]+2020x^{864}y^{1010}$$
$$+1874x^{937}y^{937}+1800x^{774}y^{900},$$

which implies that

$$D_y^2\left[\varphi_{\tilde{\mathfrak{R}}}(\zeta,x,y)\right]=x^{646}\left[1107072y^{774}+1755938y^{937}+512656y^{716}+580644y^{762}\right]$$
$$+x^{716}\left[1161288y^{762}+1492992y^{864}+599076y^{774}\right]+599076y^{774}\left[x^{762}+2x^{770}\right]$$
$$+x^{900}\left[1755938y^{937}+1897352y^{974}\right]+2040200x^{864}y^{1010}+1755938x^{937}y^{937}$$
$$+1620000x^{774}y^{900}$$

and

$$D_xD_y\varphi_{\tilde{\mathfrak{R}}}(\zeta,x,y)=646x^{646}\left[1488y^{744}+1874y^{937}+716y^{716}+762y^{762}\right]+716x^{716}\left[1524y^{762}+1728y^{864}+774y^{774}\right]$$
$$+774y^{774}\left[762x^{762}+1540x^{770}\right]+900x^{900}\left[1874y^{937}+1948y^{974}\right]+1745280x^{864}y^{1010}$$
$$+1755938x^{937}y^{937}+1393200x^{774}y^{900}.$$

The values of the $\tilde{\mathfrak{R}}$-domination topological indices obtained by substitute of $x = y = 1$ in previous calculations and from Table 1.

In the next Theorem 4.3, we compute the γ-domination topological indices via γ-polynomial.

Theorem 4.3. If ζ is the molecular graph of blue starch-iodine complex, then

1. $\varphi_\gamma(\zeta,x,y)=5+2y^8+2y^{12}+6y^{16}+2x^4y^{12}+5x^8y^8+x^8y^{16}+x^{12}y^{16}.$
2. $\gamma Z_1(\zeta)=1470,\qquad \gamma Z_2(\zeta)=736.$
   $\gamma Z_1^*(\zeta)=300,\qquad \gamma F(\zeta)=18944.$
   $\gamma H(\zeta)=5104,\qquad \gamma F^*(\zeta)=3632.$

Proof. For (1), similar steps of the proof of Theorem 3.4. For part (2), in order to find the γ-domination topological indices, we need the following calculations

$$\gamma Z_1^*(\zeta)=\left(D_x+D_y\right)\left[\varphi_\gamma(\zeta,x,y)\right]|_{x=y=1}$$
$$=16y^8+24y^{12}+96y^{16}+32x^4y^{12}+80x^8y^8+24x^8y^{16}+28x^{12}y^{16}\,|_{x=y=1}$$
$$=300.$$
$$\gamma Z_2(\zeta)=\left(D_xD_y\right)\left[\varphi_\gamma(\zeta,x,y)\right]|_{x=y=1}$$
$$=96x^4y^{12}+320x^8y^8+128x^8y^{16}+192x^{12}y^{16}\,|_{x=y=1}$$
$$=736.$$
$$\gamma F^*(\zeta)=\left(D_x^2+D_y^2\right)\left[\varphi_\gamma(\zeta,x,y)\right]|_{x=y=1}$$
$$=128y^8+288y^{12}+1536y^{16}+320x^4y^{12}+640x^8y^8+320x^8y^{16}+400x^{12}y^{16}\,|_{x=y=1}$$
$$=3632.$$

$$\gamma H(\zeta) = \left(D_x^2 + D_y^2 + 2D_xD_y\right)\left[\varphi_\gamma(\zeta, x, y)\right]|_{x=y=1}$$
$$= 128y^8 + 288y^{12} + 1536y^{16} + 512x^4y^{12} + 1280x^8y^8 + 576x^8y^{16} + 784x^{12}y^{16}\,|_{x=y=1}$$
$$= 5104$$
$$\gamma Z_1(\zeta) = \sum_{v\in V(\zeta)} d_\gamma^2 = 9(0)^2 + 2(4)^2 + 6(8)^2 + 2(12)^2 + 3(16)^2 = 1472.$$
$$\gamma F(\zeta) = \sum_{v\in V(\zeta)} d_\gamma^3 = 9(0)^3 + 2(4)^3 + 6(8)^3 + 2(12)^3 + 3(16)^3 = 18944.$$

This completes the proof.

In Figure 7, we present the 3D representation of $\varphi_{\tilde{\mathfrak{R}}}$-polynomial and φ_γ-polynomial of blue starch-iodine complex.

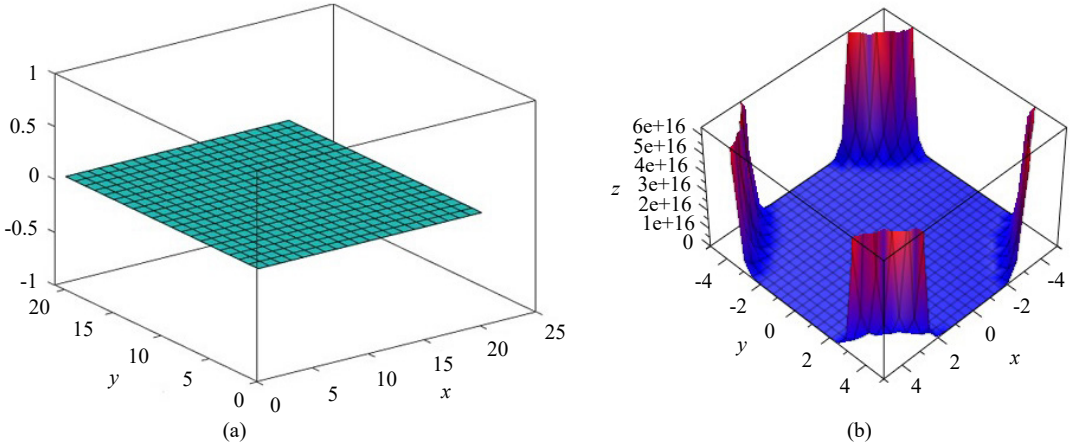

Figure 7. Plotting of (a) $\varphi_{\tilde{\mathfrak{R}}}$-polynomial; (b) φ_γ-polynomial of blue starch-iodine complex

5. Statistical validity of domination topological indices

Numerous QSPR/QSAR studies effectively use topological indexes to model the physicochemical properties of compounds based on their molecular structure. To be accepted by Randić [48], a topological index must meet certain requirements. Among these, the most significant is positively correlated with at least one property. The purpose of this section is to investigate the significance of these newly developed domination topological indices. Using the methodology developed by Vardhan et al. [49], 12 phytochemicals are screened against SARS-CoV-2 3CLpro and used in the QSPR model for predicting topological polar surface, binding energy, docking score, and molecular weight.

The correlation coefficients of computed polysaccharides and literature values in [50] and [51] are calculated. Various chemical compounds have been studied in the following experimental data [52], and also https://pubchem.ncbi.nlm.nih.gov (accessed on 26 March 2022). Chemical compounds are described in Table 11 according to their experimental data. Compound $\tilde{\mathfrak{R}}$-domination index values are shown in Table 12. Our analysis has shown that these indices play a crucial role in evaluating the topological polar surface area (*T.P.S.A.*), molecular weight (*M.W.*), complexity (*C*), boiling point (*B.P.*), and octanol-water partition coefficient (*XLogP3*) for the different chemical compounds. A correlation coefficient (*R*) between these indices and some physicochemical properties can be seen in Table 13.

Table 11. Experimental values of some physicochemical properties of some chemical compounds

Chemical compound	(*B.P.*) °C	(*C*)	(*F.P.*)	*XLogP3*	(*T.P.S.A.*) $Å^2$	(*M.W.*)
Amylose	627.7	641	333.4	6.9	269	504.4
Blue starch-iodine	/	/	/	/	/	/
Chloroquine [50]	460.6	309	232.3	4.6	28.2	319.9
Hydroxy-chloroquine [50]	516.7	331	266.3	3.6	48.4	335.9
Anthraquinone [51]	279.8	261	185	3.4	34.1	208.21
Nicotine [51]	247	147	59	1.2	16.1	162.23
Aspirin [51]	140	212	250	1.2	63.6	180.16

Table 12. Domination indices of some chemical compounds

Chemical compound	$\tilde{\Re}Z_1(\zeta)$	$\tilde{\Re}Z_2(\zeta)$	$\tilde{\Re}Z_1^*(\zeta)$	$\tilde{\Re}F(\zeta)$	$\tilde{\Re}H(\zeta)$	$\tilde{\Re}F^*(\zeta)$
Amylose	31044928	29107712	52800	3.73750×10^{10}	118138880	59923456
Blue starch-iodine	15928240	16125222	39212	$1.39011263 \times 10^{10}$	64847468	32597024
Chloroquine [50]	1811457	1728576	12627	554421762	7090227	3633075
Hydroxy-chloroquine [50]	4003420	3708635	18892	1820798614	15276248	7858978
Anthraquinone [51]	4003420	28400	1430	581576	115300	58500
Nicotine [51]	1808	1700	298	23922	6936	3536
Aspirin [51]	1041	968	223	9607	3903	1967

Table 13. Correlation coefficients (*R*) between domination indices and some physiochemical properties of some chemical compounds

$\tilde{\Re}$-domination index	(*B.P.*) °C	(*C*)	(*F.P.*)	*XLogP3*	(*T.P.S.A.*) $Å^2$	(*M.W.*)
$\tilde{\Re}Z_1(\zeta)$	0.710	0.954	0.646	0.816	0.981	0.888
$\tilde{\Re}Z_2(\zeta)$	0.709	0.954	0.645	0.817	0.981	0.888
$\tilde{\Re}Z_1^*(\zeta)$	0.839	0.979	0.724	0.889	0.919	0.973
$\tilde{\Re}F(\zeta)$	/	/	/	/	/	/
$\tilde{\Re}H(\zeta)$	0.710	0.954	0.646	0.817	0.981	0.888
$\tilde{\Re}F^*(\zeta)$	0.711	0.955	0.647	0.818	0.981	0.889

5.1 *Results and discussion*

On the basis of the data in Tables 11 and 12, a linear regression model was developed for the topological polar surface area (*T.P.S.A.*), molecular weight (*M.W.*), complexity (*C*), boiling point (*B.P.*), and octanol-water partition coefficient *(XLogP3*). Our linear regression model is as follows: $P = A + B(DI)$ where P = physical property and DI = domination index. R was calculated correspondingly. Based on the data in Table 13, some results can be derived for the new $\tilde{\Re}$-domination topological indices given (except for the forgotten domination index, $\tilde{\Re}F(\zeta)$ which will not be discussed). A regression model is shown in this table for various physicochemical properties. As can be seen, R is greater than 0.645 in the regression model.

Hence, the defined new $\tilde{\Re}$-domination topological indices correlate positively with all the physical and chemical properties of the different chemical compounds. To begin with, it was discovered that any structure-property relationship could not be achieved using the forgotten domination index $\tilde{\Re}F(\zeta)$. Modified domination Zagreb index $\tilde{\Re}Z_1^*(\zeta)$ demonstrates that this index is a powerful tool for determining physical and chemical properties of different chemical compounds under this study, with correlation coefficients ranging from 0.724 to 0.979. According to the table, when we examine the correlation coefficients horizontally for physical properties, we see that $\tilde{\Re}Z_1^*(\zeta)$ index gives the highest correlation coefficient for boiling point (*B.P.*) (R = 0.839), complexity (*C*) (R = 0.979), flash point (*F.P.*) (R = 0.724),

octanol-water partition coefficient (*XLogP3*) ($R = 0.889$), and molecular weight (*M.W.*) ($R = 0.973$).

As a result, QSPR/QSAR can be predicted from the modified domination Zagreb index $\tilde{\Re}Z_1^*(\zeta)$ for a wide variety of chemical compounds. The topological polar surface area (*T.P.S.A.*) properties are correctly predicted using these $\tilde{\Re}$-domination topological indices. The range of the correlation coefficient is between 0.919 and 0.981. According to all domination topological indices, the molecular weight (*M.W.*) is predicted with a high correlation coefficient between 0.888 and 0.973. In a similar range, complexity (*C*) $0.954 \leq R \leq 0.979$ can also be found.

In Figure 8, the correlation coefficient R values are displayed with the different domination topological indices. These chemical compounds may not be suitable for predicting the efficiency of the γ-dominations since the correlation coefficient R was not satisfactory. This may indicate that topological indices based on *M.D.S.* are more powerful than those based on *m.d.s*. Despite this, we believe it is well justified to raise concerns about more different compounds.

This paper reconstructs the topological indices of domination ($\tilde{\Re}$-domination topological indices and γ-dominations topological indices) via new polynomials ($\varphi_{\tilde{\Re}}$-polynomial and φ_{γ}-polynomial), and finds their exact values over polysaccharides: amylose and blue starch-iodine complex.

A QSPR was performed to assess the efficacy of the calculated domination topological indices against the physicochemical properties of amylose as well as nicotine, aspirin, chloroquine, hydroxychloroquine, and anthraquinone. According to this QSPR study, various domination topological indices computed in this article are highly predictive of physicochemical properties. With the help of these domination topological indices, future calculations could involve more complex compounds.

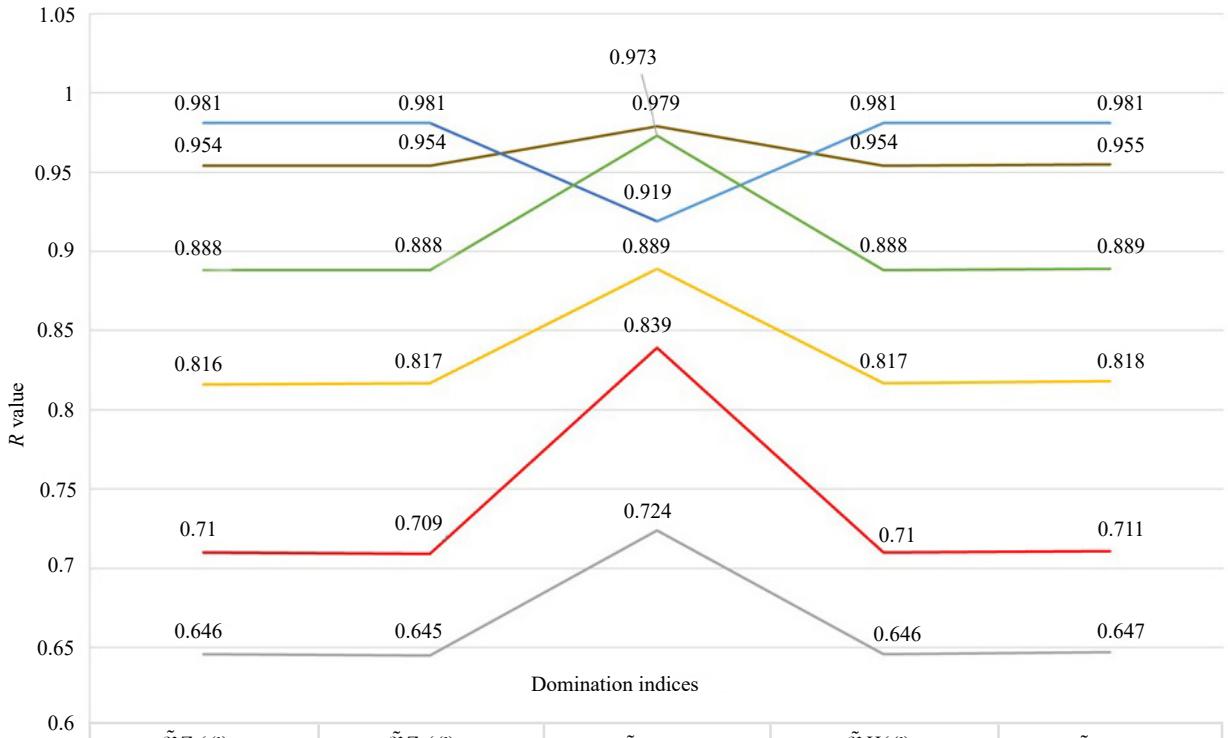

	$\tilde{\Re}Z_1(\zeta)$	$\tilde{\Re}Z_2(\zeta)$	$\tilde{\Re}Z_1^*(\zeta)$	$\tilde{\Re}H(\zeta)$	$\tilde{\Re}F^*(\zeta)$
(*B.P.*)	0.71	0.709	0.839	0.71	0.711
(*C*)	0.954	0.954	0.979	0.954	0.955
(*F.P.*)	0.646	0.645	0.724	0.646	0.647
XLogP3	0.816	0.817	0.889	0.817	0.818
(*T.P.S.A*)	0.981	0.981	0.919	0.981	0.981
(*M.W.*)	0.888	0.888	0.973	0.888	0.889

Figure 8. Correlation coefficient values for the domination topological indices

6. Conclusion

In the intricate realm of molecular structures, topological indices have emerged as indispensable tools for unraveling the structural and physicochemical intricacies of polysaccharides, notably amylose and blue starch-iodine compounds. Our research has addressed the long-standing challenge of accurately determining these indices across diverse isomeric forms. By introducing these innovative polynomials methodologies, we have not only catered to both chair and boat isomeric forms but also seamless integrated advanced computational techniques, specifically DFT calculations, within the Gaussian 09 software framework.

Our rigorous validation process, encompassing a QSPR analysis and benchmarking against well-established compounds such as nicotine and aspirin, has unequivocally demonstrated the robustness and precision of our approach. The compelling correlations we observed between topological indices and the inherent properties of the compounds underscore the potential of our methodology as a reliable and versatile tool. In essence, this study has significantly enriched our understanding of polysaccharides, paving the way for groundbreaking applications in diverse sectors, including pharmaceuticals, materials science, and agriculture.

The insights gleaned from our research not only hold promise for a deeper comprehension of these complex molecules but also beckon a new era of innovation, where the design of novel polysaccharides with bespoke properties becomes a tangible reality.

Data availability

The authors confirm that the data supporting the findings of this study are available within the article.

Author contributions

Suha Wazzan: conceptualization, methodology, validation, formal analysis, investigation, writing-original draft, preparation, writing-review and editing, supervision, project administration, funding acquisition. Hanan Ahmed: conceptualization, validation, investigation, resources, data curation, writing-review and editing. All authors have read and agreed to the published version of the manuscript.

Conflict of interest

The authors declare that they have no conflict of interest.

Acknowledgments

Thanks to Prof. Nuha Wazzan from Chemistry department, King Abdulaziz University, Jeddah, Saudi Arabia, for carrying out the DFT calculations. Authors are thankful for King Abdulaziz University's High-Performance Computing Centre (Aziz Supercomputer) (http://hpc.kau.edu.sa) for supporting the computation for the work described in this paper.

References

[1] Jensen F. *Introduction to computational chemistry*. 3rd ed. West Sussex, UK: John Wiley & Sons; 2017.

[2] Stephen AM, Phillips GO. *Food polysaccharides and their applications*. 2nd ed. Boca Raton, Florida: CRC Press; 2016.

[3] Green MM, Blankenhorn G, Hart H. Which starch fraction is water-soluble, amylose or amylopectin? *Journal of Chemical Education*. 1975; 52(11): 729-730. Available from: https://doi.org/10.1021/ed052p729.

[4] Rosciardi V. Baglioni P. Role of amylose and amylopectin in PVA-starch hybrid cryo-gels networks formation

from liquid-liquid phase separation. *Journal of Colloid and Interface Science*. 2023; 630: 415-425. Available from: https://doi.org/10.1016/j.jcis.2022.10.092.

[5] Pérez S, Mazeau K, Du Penhoat CH. The three-dimensional structures of the pectic polysaccharides. *Plant Physiology and Biochemistry*. 2000; 38(1-2): 37-55. Available from: https://doi.org/10.1016/S0981-9428(00)00169-8.

[6] Haynes TW, Hedetniemi ST, Henning MA. Domination in diagraphs. In: Haynes TW, Hedetniemi ST, Henning MA. (eds.) *Structures of domination in graphs*. Developments in Mathematics, vol 66. Cham: Springer; 2021. p.387-428. Available from: https://doi.org/10.1007/978-3-030-58892-2_13.

[7] Das KC, Çevik AS, Cangul IN, Shang Y. On Sombor index. *Symmetry*. 2021; 13(1): 140. Available from: https://doi.org/10.3390/sym13010140.

[8] Demirci M, Delen S, Cevik AS, Cangul IN. Omega index of line and total graphs. *Journal of Mathematics*. 2021; 2021: 5552202. Available from: https://doi.org/10.1155/2021/5552202.

[9] Hayat S, Khan S. Quality testing of spectrum-based valency descriptors for polycyclic aromatic hydrocarbons with applications. *Journal of Molecular Structure*. 2021; 1228: 129789. Available from: https://doi.org/10.1016/j.molstruc.2020.129789.

[10] Wazzan S, Saleh A. New versions of locating indices and their significance in predicting the physicochemical properties of benzenoid hydrocarbons. *Symmetry*. 2022; 14(5): 1022. Available from: https://doi.org/10.3390/sym14051022.

[11] Wazzan S, Saleh A. Locating and multiplicative locating indices of graphs with QSPR analysis. *Journal of Mathematics*. 2021; 2021: 5516321. Available from: https://doi.org/10.1155/2021/5516321.

[12] Wazzan S, Ahmed H. Symmetry-adapted domination indices: The enhanced domination sigma index and its applications in QSPR studies of octane and its isomers. *Symmetry*. 2023; 15(6): 1202. Available from: https://doi.org/10.3390/sym15061202.

[13] Haynes T. *Domination in graphs*. Volume 2: Advanced Topics. New York: Routledge; 2017. Available from: https://doi.org/10.1201/9781315141428.

[14] Ahangar HA, Chellali M, Sheikholeslami SM, Valenzuela-Tripodoro JC. Maximal double Roman domination in graphs. *Applied Mathematics and Computation*. 2022; 414: 126662. Available from: https://doi.org/10.1016/j.amc.2021.126662.

[15] Abdlhusein MA, Al-Harere MN. New parameter of inverse domination in graphs. *Indian Journal of Pure and Applied Mathematics*. 2021; 52(1): 281-288. Available from: https://doi.org/10.1007/s13226-021-00082-z.

[16] Raju S, Nayaka SR. On the second domination hyper index of graph and some graph operations. *Advances and Applications in Discrete Mathematics*. 2023; 39(1): 125-143. Available from: https://doi.org/10.17654/0974165823041.

[17] Bousquet N, Deschamps Q, Lehtilä T, Parreau A. Locating-dominating sets: From graphs to oriented graphs. *Discrete Mathematics*. 2023; 346(1): 113124. Available from: https://doi.org/10.1016/j.disc.2022.113124.

[18] Shashidhara AA, Ahmed H, Nandappa S, Cancan M. Domination version: Sombor index of graphs and its significance in predicting physicochemical properties of butane derivatives. *Eurasian Chemical Communications*. 2023; 5(1): 91-102. Available from: https://doi.org/10.22034/ecc.2023.357241.1522.

[19] Ahmad M, Saeed M, Arshad M, Cheema IZ, Hussain M. Algebraic polynomials and invariants of certain chemical networks. *Journal of Computational and Theoretical Nanoscience*. 2018; 15(4): 1340-1347. Available from: https://doi.org/10.1166/jctn.2018.7312.

[20] Diudea MV. Omega polynomial. *Carpathian Journal of Mathematics*. 2006; 22(1-2): 43-47. Available from: https://www.carpathian.cunbm.utcluj.ro/article/omega-polynomial/.

[21] Diudea MV, Simona C, Peter EJ. Omega and related counting polynomials. *MATCH Communications in Mathematical and in Computer Chemistry*. 2008; 60(1): 237-250. Available from: https://match.pmf.kg.ac.rs/electronic_versions/Match60/n1/match60n1_237-250.pdf.

[22] Knor M, Tratnik N. A new alternative to Szeged, Mostar, and PI polynomials-The SMP polynomials. *Mathematics*. 2023; 11(4): 956. Available from: https://doi.org/10.3390/math11040956.

[23] Chou CP, Witek HA. Closed-form formulas for the Zhang-Zhang polynomials of benzenoid structures: Chevrons and generalized chevrons. *MATCH Communications in Mathematical and in Computer Chemistry*. 2014; 72(1):

105-124. Available from: https://match.pmf.kg.ac.rs/electronic_versions/Match72/n1/match72n1_105-124.pdf.
[24] Balasubramanian K. Topological indices, graph spectra, entropies, Laplacians, and matching polynomials of n-dimensional hypercubes. *Symmetry*. 2023; 15(2): 557. Available from: https://doi.org/10.3390/sym15020557.
[25] Ibrahim M, Husain S, Zahra N, Ahmad A. Vertex-edge degree based indices of honey comb derived network. *Computer Systems Science Engineering*. 2022; 40(1): 247-258. Available from: https://doi.org/10.32604/CSSE.2022.018227.
[26] Masmali I, Nadeem M, Yousaf A, Akbar A, Razaq A, Razzaque A. An effective technique for developing the graphical polynomials of certain molecular graphs. *Scientific Reports*. 2023; 13(1): 4764. Available from: https://doi.org/10.1038/s41598-023-31623-7.
[27] Chen H. The Tutte polynomial of a class of compound graphs and its applications. *Discrete Mathematics, Algorithms and Applications*. 2023; 15(01): 2250058. Available from: https://doi.org/10.1142/S1793830922500586.
[28] Aziz A, Mohammed HN, Ali AM. Schultz and modified Schultz polynomials of edges induce chain and ring for hexagonal graphs. *European Journal of Pure and Applied Mathematics*. 2023; 16(3): 1580-1591. Available from: https://doi.org/10.29020/nybg.ejpam.v16i3.4783.
[29] Ali AM, Abdullah HO, Saleh GAM. Hosoya polynomials and Wiener indices of carbon nanotubes using mathematica programming. *Journal of Discrete Mathematical Sciences and Cryptography*. 2022; 25(1): 147-158. Available from: https://doi.org/10.1080/02522667.2021.1968578.
[30] Wiener H. Structural determination of paraffin boiling points. *Journal of the American Chemical Society*. 1947; 69(1947): 17-20. Available from: https://doi.org/10.1021/ja01193a005.
[31] Cash GG. Relationship between the Hosoya polynomial and the hyper-Wiener index. *Applied Mathematics Letters*. 2002; 15(7): 893-895. Available from: https://doi.org/10.1016/S0893-9659(02)00059-9.
[32] Afzal F, Hussain S, Afzal D, Razaq S. Some new degree based topological indices via M-polynomial. *Journal of Information and Optimization Sciences*. 2020; 41(4): 1061-1076. Available from: https://doi.org/10.1080/02522667.2020.1744307.
[33] Deutsch E, Klavžar S. M-polynomial and degree-based topological indices. *ArXiv* [Preprint] 2014. Version 1. Available from: https://doi.org/10.48550/arXiv.1407.1592.
[34] Rai S, Das S. M-polynomial and degree-based topological indices of subdivided chain hex-derived network of type 3. In: Woungang I, Dhurandher SK, Pattanaik KK, Verma A, Verma P. (eds.) *Advanced Network Technologies and Intelligent Computing*. ANTIC 2021. Communications in Computer and Information Science, vol 1534. Cham: Springer; 2021. p.410-424. Available from: https://doi.org/10.1007/978-3-030-96040-7_33.
[35] Rasool KB, Rashed PA, Ali AM. Relations between vertex-edge degree based topological indices and M_{ve} -polynomial of *r*-regular simple graph. *European Journal of Pure and Applied Mathematics*. 2023; 16(2): 773-783. Available from: https://doi.org/10.29020/nybg.ejpam.v16i2.4698.
[36] Afzal D, Ali S, Afzal F, Cancan M, Ediz S, Farahani MR. A study of newly defined degree-based topological indices via M-polynomial of Jahangir graph. *Journal of Discrete Mathematical Sciences and Cryptography*. 2021; 24(2): 427-438. Available from: https://doi.org/10.1080/09720529.2021.1882159.
[37] Halder D, Das S, Joseph A, Jeyaprakash RS. Molecular docking and dynamics approach to in silico drug repurposing for inflammatory bowels disease by targeting TNF alpha. *Journal of Biomolecular Structure and Dynamics*. 2023; 41(8): 3462-3475. Available from: https://doi.org/10.1080/07391102.2022.2050948.
[38] Ullah A, Zeb A, Zaman S. A new perspective on the modeling and topological characterization of H-naphtalenic nanosheets with applications. *Journal of Molecular Modeling*. 2022; 28(8): 211. Available from: https://doi.org/10.1007/s00894-022-05201-z.
[39] Khabyah AA, Zaman S, Koam AN, Ahmad A, Ullah A. Minimum Zagreb eccentricity indices of two-mode network with applications in boiling point and benzenoid hydrocarbons. *Mathematics*. 2022; 10(9): 1393. Available from: https://doi.org/10.3390/math10091393.
[40] Yan T, Kosar Z, Aslam A, Zaman S, Ullah A. Spectral techniques and mathematical aspects of K_4 chain graph. *Physica Scripta*. 2023; 98(4): 045222. Available from: https://doi.org/10.1088/1402-4896/acc4f0.
[41] Zaman S, Jalani M, Ullah A, Saeedi G. Structural analysis and topological characterization of Sudoku nanosheet. *Journal of Mathematics*. 2022; 2022: 5915740. Available from: https://doi.org/10.1155/2022/5915740.
[42] Leemhuis H, Pijning T, Dobruchowska JM, Van Leeuwen SS, Kralj S, Dijkstra BW, et al. Glucansucrases: Three-

dimensional structures, reactions, mechanism, α-glucan analysis and their implications in biotechnology and food applications. *Journal of Biotechnology*. 2013; 163(2): 250-272. Available from: https://doi.org/10.1016/j.jbiotec.2012.06.037.

[43] Tao J, Perdew JP, Staroverov VN, Scuseria GE. Climbing the density functional ladder: Nonempirical meta-generalized gradient approximation designed for molecules and solids. *Physical Review letters*. 2003; 91(14): 146401. Available from: https://doi.org/10.1103/PhysRevLett.91.146401.

[44] Dunning Jr TH. Gaussian basis sets for use in correlated molecular calculations. I. The atoms boron through neon and hydrogen. *The Journal of Chemical Physics*. 1989; 90(2): 1007-1023. Available from: https://doi.org/10.1063/1.456153.

[45] Frisch MJ, Nielsen AB, Hratchian HP. *Gaussian 09 programmer's reference*. Wallingford: Gaussian Inc; 2009.

[46] Dennington R, Keith T, Millam J. *GaussView*. (Version 5.0.8) [Software] Shawnee Mission, KS: Semichem Inc. 2009.

[47] Koopmans T. Über die zuordnung von wellenfunktionen und eigenwerten zu den einzelnen elektronen eines atoms. *Physica*. 1934; 1(1-6): 104-113. Available from: https://doi.org/10.1016/S0031-8914(34)90011-2.

[48] Randić M. Generalized molecular descriptors. *Journal of Mathematical Chemistry*. 1991; 7(1): 155-168. Available from: https://doi.org/10.1007/BF01200821.

[49] Vardhan S, Sahoo SK. In silico ADMET and molecular docking study on searching potential inhibitors from limonoids and triterpenoids for COVID-19. *Computers in Biology and Medicine*. 2020; 124: 103936. Available from: https://doi.org/10.1016/j.compbiomed.2020.103936.

[50] Ahmed H, Alwardi A, Salestina MR, Nandappa DS. Domination, γ-domination topological indices and φ_P-polynomial of some chemical structures applied for the treatment of COVID-19 patients. *Biointerface Research in Applied Chemistry*. 2021; 11(5): 13290-13302. Available from: https://doi.org/10.33263/BRIAC115.1329013302.

[51] Ahmed H, Raghavachar R, Alameri A, Morgan RS. Computation domination and γ-domination topological indices of hexane isomers via φ_P-polynomial with QSPR Analysis. *Biointerface Research in Applied Chemistry*. 2022; 13(2): 182. Available from: https://doi.org/10.33263/BRIAC132.182.

[52] Das S, Rai S, Mandal M. M-polynomial and correlated topological indices of antiviral drug molnupiravir used as a therapy for COVID-19. *Polycyclic Aromatic Compounds*. 2022; 43(8): 7027-7041. Available from: https://doi.org/10.1080/10406638.2022.2131854.